JOURNAL OF MATERIALS SCIENCE 30 (1995) 3936–3943

Synthesis of $Pb(Mg_{1/3}Nb_{2/3})\ O_3$ perovskite by an alkoxide method

JANG-CHENG HO, KUO-SHUNG LIU, I-NAN LIN*
*Department of Materials Science and Engineering, *Materials Science Center, National Tsing-Hua University, Hsinchu 30043, Taiwan*

$Pb(Mg_{1/3}Nb_{2/3})O_3$ materials have been synthesized using sol–gel, freeze-drying or spray-pyrolysis techniques. The as-prepared powders were of an amorphous form which could be converted into a crystalline form by calcination. The pyrochlore phase was inevitably formed with an accompanying perovskite phase. As the calcining temperature increased, greater proportions of the desired perovskite phase occurred. The residual pyrochlore phase could be completely transformed into the perovskite phase when the powders were prepared via freeze-drying or by a spray-pyrolysis method. The maximum proportion of the pyrochlore phase was, however, only 92% when the powders were synthesized by a sol–gel route. Thermal gravimetric analysis/differential thermal analysis (TGA/DTA) and infrared transmission spectroscopy (FTIR) indicated that $Mg(OEt)_2$ and $Nb(OEt)_5$ formed a double alkoxide but $Pb(OAc)_2$ formed separate clusters during the hydrolysis of the solution in the sol–gel process. Inhomogeneous mixing meant that the intermediate phase formed was rather difficult to eliminate completely. Homogeneous mixing was preserved when the solution was directly freeze dried or spray pyrolysed. The size of the preferentially formed pyrochlore phase was very fine and further transformation was feasible. $Pb(Mg_{1/3}Nb_{2/3})O_3$ materials, free of the pyrochlore phase, could therefore be obtained.

1. Introduction

Lead-magnesium niobate (PMN), $Pb(Mg_{1/3}Nb_{2/3})\ O_3$, with a perovskite $A(B',B'')O_3$ structure, exhibits excellent physical properties such as a high dielectric constant [1–3], a large electrostrictivity [2, 4–7], a low thermal expansion and diffuse-phase-transition (DPT) characteristics [8, 9]. These occur near the Curie temperature (T_c). The non-hysteresis electrostrictive properties [10] make them the best candidates for transducers where precision in the displacement of submicrometre order is required.

Synthesis of PMN by a mixed-oxide method is, however, difficult owing to the inevitable formation of the unwanted pyrochlore phase. The kinetics for the conversion of the pyrochlore phase to perovskite are rather slow and necessitate firing for prolonged periods at an elevated temperature. Repeated processing steps are still, however, required despite the fact that the intermediate-compound methods previously proposed by Lejeune and Boilot [11], Swartz and Shrout [12], or Guha and Anderson [13] have successfully synthesized pyrochlore-free PMN materials.

On the other hand, powder preparation from organic solutions [14, 15] is a technique currently being used which offers several advantages such as ease of preparation of the solution, close control of the purity level and marvelous compositional homogeneity. The merits and mechanisms of synthesizing powders from polymeric precursors have been thoroughly reviewed [16]. The preparation of the PMN powders has, however, not been as successful as initially expected. Significant amounts of pyrochlore phase still remained when the PMN powders were prepared via the conventional sol-gel route [17–19]. Pyrochlore-phase-free PMN powder can only be obtained when a special process such as seeding [20] or hypercritical aerogeling [21] is adapted.

This investigation used direct synthesis from solution (DSS) techniques such as freeze-drying and spray-pyrolysis methods to prepare a pyrochlore-free PMN phase. The characteristics of materials made this way are examined extensively and compared to those of sol–gel-derived powders and ceramics. The mechanism which results in a different behaviour of the powders prepared by the sol–gel method is also investigated.

2. Experimental procedure

PMN powders were prepared via either sol–gel, freeze-drying or spray-pyrolysis techniques. The experimental procedure included two major steps; namely, the preparation of a PMN solution and the synthesis of PMN powders. The niobium pentaethoxide, $Nb(OC_2H_5)_5$, required for all the three methods was first prepared, following the process developed by Bradley *et al.* [22], and described by the following

0022–2461 © *1995 Chapman & Hall*

reaction:

$$NbCl_5 + 5C_2H_5OH + 5(C_2H_5)_3N \xrightarrow{10\,^{\circ}C} Nb(OC_2H_5)_5 + 5(C_2H_5)_3NHCl \downarrow$$

2.1. The sol–gel process

Magnesium ethoxide, $Mg(OC_2H_5)_2$ (Aldrich Chemical Company Inc., WI, USA), niobium ethoxide, $Nb(OC_2H_5)_5$, and lead-acetate trihydrate, $Pb(CH_3COO)_2 \cdot 3H_2O$ (Merck Company, Darmstadt, FRG), were used as starting materials for the preparation of a complex alkoxide solution. A Mg–Nb mixture was prepared by refluxing the Mg and Nb alkoxides, in a 1 : 2 molar ratio, in 2-methoxyethanol. A Pb solution was separately prepared by dissolving the lead-acetate trihydrate in 2-methoxyethanol, and then heating it at 124 °C to remove hydrated water. The two solutions in a proper cationic ratio, were mixed together then hydrolysed with a sufficient amount of water (H_2O : Nb $(OC_2H_5)_5 = 5 : 1$). The gels obtained were dried and then calcined at 700 ~ 1000 °C to convert the PMN precursors into powders.

2.2. The freeze-drying process

The $Nb(OEt)_5$ was first stabilized by oxalic acid, following the technique proposed by Koichi [23]. The molar ratio of $Nb(OEt)_5$ to $H_2C_2O_4 \cdot 2H_2O$ was 1 : 2.7. $Pb(CH_3COO)_2 \cdot 3H_2O_{(aq)}$ (0.1 M) and HNO_3 (65%) were then alternately added to the stabilized $Nb(OEt)_5$ solution, with the solution temperature kept below 35 °C during the dissolving process to prohibit the evolution of NO_2 gas. A suitable amount of $Mg(CH_3COO)_2 \cdot 4H_2O_{(s)}$ (Merck Company, Darmstadt, FRG) was finally added, producing a clear PMN solution of stoichiometric composition. The aqueous PMN solution was carried by nitrogen gas and nozzle sprayed into liquid nitrogen. The frozen droplets of PMN were then heated rather slowly to 30 °C in a low-pressure chamber($\sim 10^{-1}$ Pa) to sublimate the solvents; this was followed by calcining at 800 ~ 875 °C for 4 h.

2.3. Spray pyrolysis

The $Nb(OEt)_5$ was alternatively stabilized following the Pechini method [24], by a polyester solvent which was obtained by dissolving 1 g of citric acid ($C_6H_8O_7 \cdot H_2O$) in 8 cm^3 of ethylene glycol ($C_2H_6O_2$) at 90 °C ~ 100 °C. The correct amounts of $Pb(Ch_3COO)_2 \cdot 3H_2O$, and $Mg(CH_3COO)_2$ $4H_2O_{(s)}$, were finally added simultaneously to the polyester-stabilized $Nb(OEt)_5$ to yield a clear, yellowish, PMN solution. This solution was then sprayed into a quartz tube (of 100 mm outside diameter, and 1000 mm length) and maintained at 700 ~ 900 °C, through use of a pneumatic nozzle. N_2 gas was chosen as a carrier gas to prevent a possible violent reaction due to carbon–oxygen or hydrogen–oxygen reactions at high temperatures. This choice was made since large amounts of carbon and hydrogen were contained in the acetate/polyester PMN solution. The powders were collected from the exhaust end of the quartz tube using a flask and then calcined at 800 or 900 °C for 4 h.

The same ceramic processes, including pulverization, pelletization and sintering at 1000 ~ 1200 °C for 4 h, were used for preparation of PMN-sintered samples from all the three kinds of PMN powders. The crystallinity and phase composition of the powders, obtained either by sol–gel, freeze-drying or spray-pyrolysis techniques, were determined using X-ray diffraction (XRD) techniques (Siemens D500). The particle morphology was examined using scanning electron microscopy (SEM). The crystal structure and microstructure of the sintered samples were also determined using XRD and SEM respectively. The decomposition characteristics of the sol-gel and spray-pyrolysed powders were examined using TGA (TGA, ULVAC-TGD7000) and DTA (ULVAC TGD-7000). The infrared transmission spectra of the sol–gel-derived powder were measured using FTIR (BOMEM, MB-100).

3. Results

The powders derived from sol–gel processes, have been indicated, by the XRD pattern shown in Fig. 1, to have an amorphous form. These powders transformed into a crystalline form when calcined. Only pyrochlore (π) was observed for powders calcined at 700 °C, which indicates a strong tendency to form a $Pb_2Nb_2O_7$ (π) phase. The perovskite phase, $Pb(Mg_{1/3}Nb_{2/3})O_3$, can only be obtained by calcining the sol–gel-derived powders at a temperature of 800 °C or higher. For higher

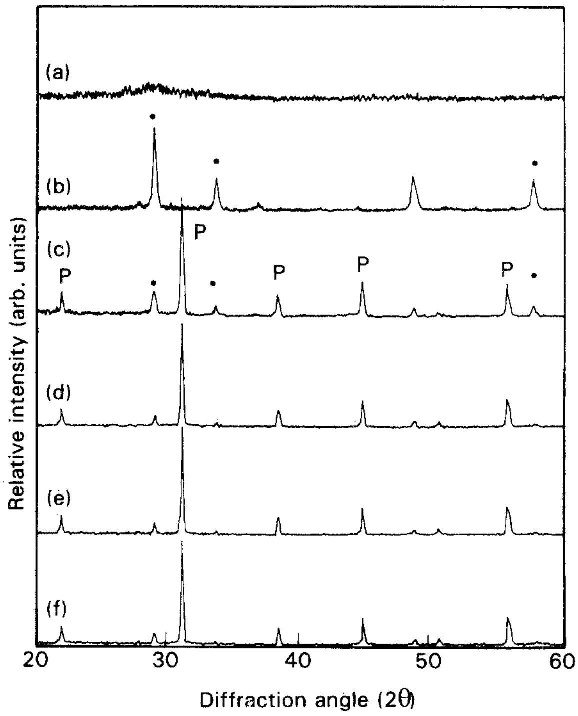

Figure 1 XRD patterns of sol–gel-derived powders: (a) as-dried, (b) calcined at 700 °C, (c) calcined at 800 °C, (d) calcined at 900 °C, (e) calcined at 1000 °C, and (f) calcined at 800 °C then sintered at 1200 °C for 4 h. (P) and (●) denote perovskite and pyrochlore, respectively.

calcination temperatures, higher proportions of perovskite phase occur; the pyrochlore phase can, however, never be completely eliminated. The maximum content of the perovskite phase is 92% when prepared via a sol–gel route. The same phenomenon has also been previously reported by several investigators [17–19]. The calcined powders were highly agglomerated, of a size around a few micrometres (Fig. 2a). The microstructure of the samples sintered at 1200 °C is shown in Fig. 2b to be quite uniform (~5 μm), but the pyrochlore phase (π) could not be completely transformed into the perovskite phase (see Fig. 1).

The powders obtained from the freeze-dried process were loose and uniform and were readily wettable when exposed to a high-humidity atmosphere. They were of an acetate mixture. The desired perovskite phase was obtained with appreciable amounts of the pyrochlore (π) phase coexisting, when the powder was calcined. A lower pyrochlore content was retained, again, when the calcination temperature was increased, as shown in Fig. 3a to c for those powders calcined at 800 °C, 850 °C and 875 °C. The calcined powders shown in Fig. 4a were very fine and uniform (~1 μm) but were agglomerated (~10 μm) when calcined at 800 °C. The grain size of the sintered specimens is indicated by the micrographs shown in Fig. 4b to be rather uniform (~8 μm). The sintered density is around 90–93% of theoretical density (TD). The minor amounts of the pyrochlore phase observed had transformed into the perovskite phase when the 800 °C calcined powders were pulverized, pressed into pellets and sintered at 1100 °C for 4 h. (Compare Fig. 3a to d). The characteristics of the samples pressed from powders calcined at 850 or 875 °C were the same as those of the samples made from powders calcined at 800 °C. They were of pure perovskite phase and of a similar granular structure (Fig. 4c and d). That is, pyrochlore-free perovskite PMN bulk materials could be obtained by sintering the powders derived from the freeze-drying technique at a temperature as low as 1100 °C. The amount of pyrochlore phase remaining in the calcined powders did not exert a significant effect upon the purity of the phase of the sintered samples.

As to the characteristics of the powders prepared by the spray-pyrolysis technique, a broadened peak corresponding to the pyrochlore phase was observed for those powders which were spray-pyrolysed at 900 °C (Fig. 5a). The powders were mostly of amorphous form with no perovskite signal observable at all. The as-sprayed powders were black in colour, presumably because of the charred hydrocarbon contained in the PMN solution. The actual temperature experienced by the atomized mists was inferred from this charred hydrocarbon to probably be below the hot-zone temperature because the droplets resided for an insufficiently short interval in this zone. The colour of the powders was converted into a yellowish colour when they were calcined at 800 °C for 4 h. These powders are illustrated in Fig. 5b to be the desired perovskite phase containing a small amount of the pyrochlore phase (π). The π-particles were completely eliminated when calcined at 900 °C for 4 h (Fig. 5c). The characteristics of the powders spray pyrolysed at 700 °C were

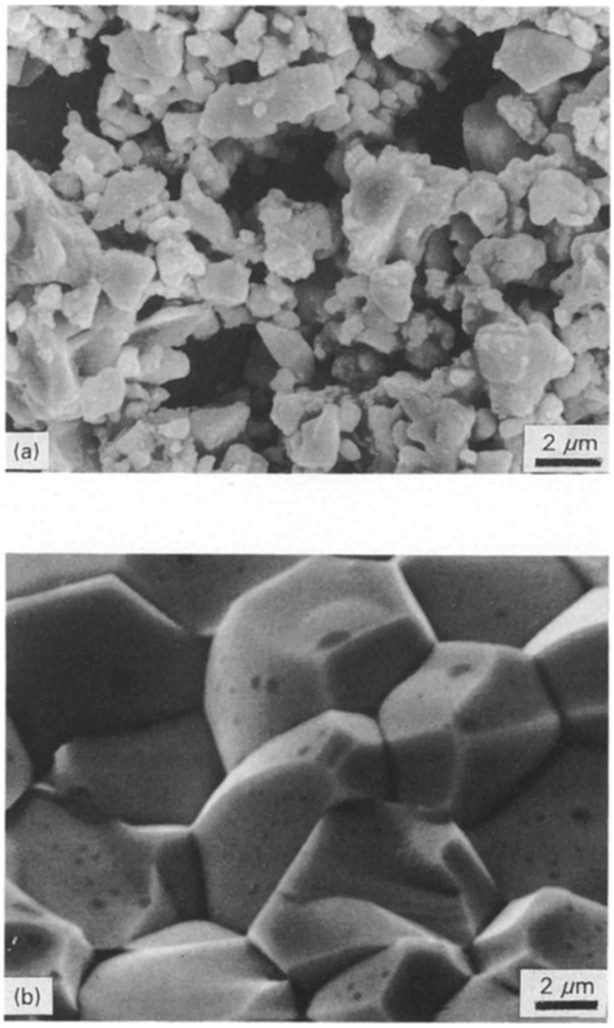

Figure 2 The microstructure of sol–gel-derived powders: (a) calcined at 800 °C, and then (b) sintered at 1200 °C for 4 h.

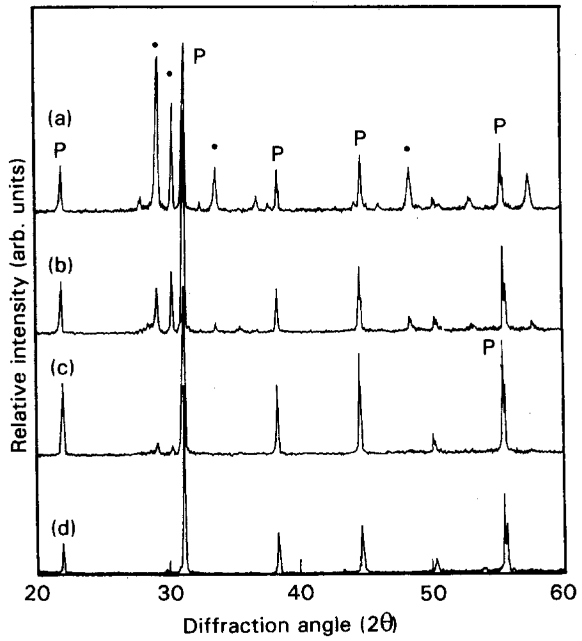

Figure 3 XRD patterns of freeze-dried-derived powders calcined at: (a) 800 °C, (b) 850 °C, (c) 875 °C, and (d) 875 °C followed by sintering at 110 °C for 4 h. (P) and (●) denote perovskite and pyrochlore, respectively.

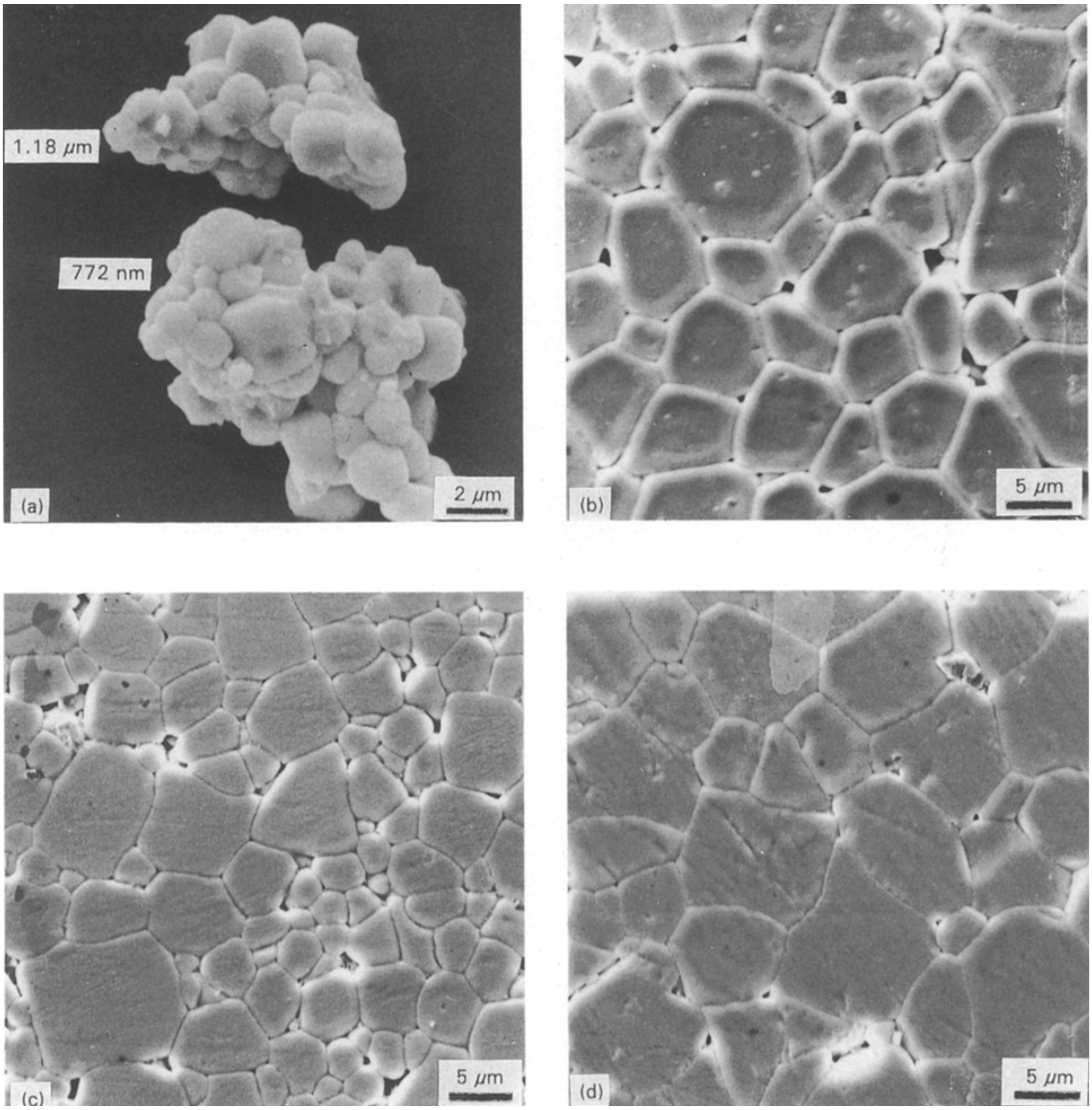

Figure 4 The microstructure of: (a) the typical morphology of the calcined powders; and the pellets sintered at 1100 °C made from freeze-dried powders calcined for 4 h at (b) 800 °C, (c) 850 °C, and (d) 875 °C.

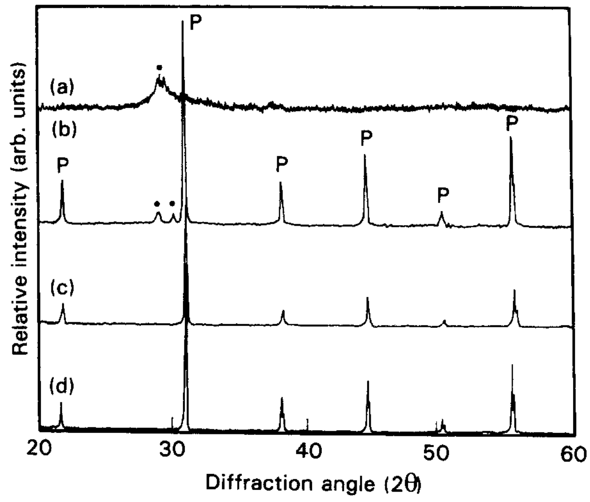

Figure 5 XRD patterns of powders spray pyrolysed at 900 °C: (a) as-sprayed, (b) calcined at 800 °C for 4 h, (c) calcined at 900 °C for 4 h, and (d) sintered at 1100 °C for 4 h. (P) and (●) denote perovskite and pyrochlore, respectively.

precisely the same as those prepared at 900 °C. That is, the amorphous phase for the as-sprayed powder could be completely converted into a crystalline PMN perovskite phase when properly calcined.

The as-sprayed powders were of a hollow, spherical, geometrical shape around 16 ~ 23 μm in size, and the calcined powders are shown in the micrographs of Fig. 6a and b to be agglomerates of a size around 15 μm. The particles in the agglomerates are, however, of submicrometre size. The spherical geometrical shape and porous nature of the as-sprayed powders indicated that the powders were actually derived from the atomized droplets. The organic materials contained in the as-sprayed powders would decompose first during the calcining process. Necking between the particles occurred during the crystallization process so that large agglomerates consisting of submicrometre grains resulted. The pyrochlore-free perovskite structure is indicated by the XRD pattern shown in Fig. 5d

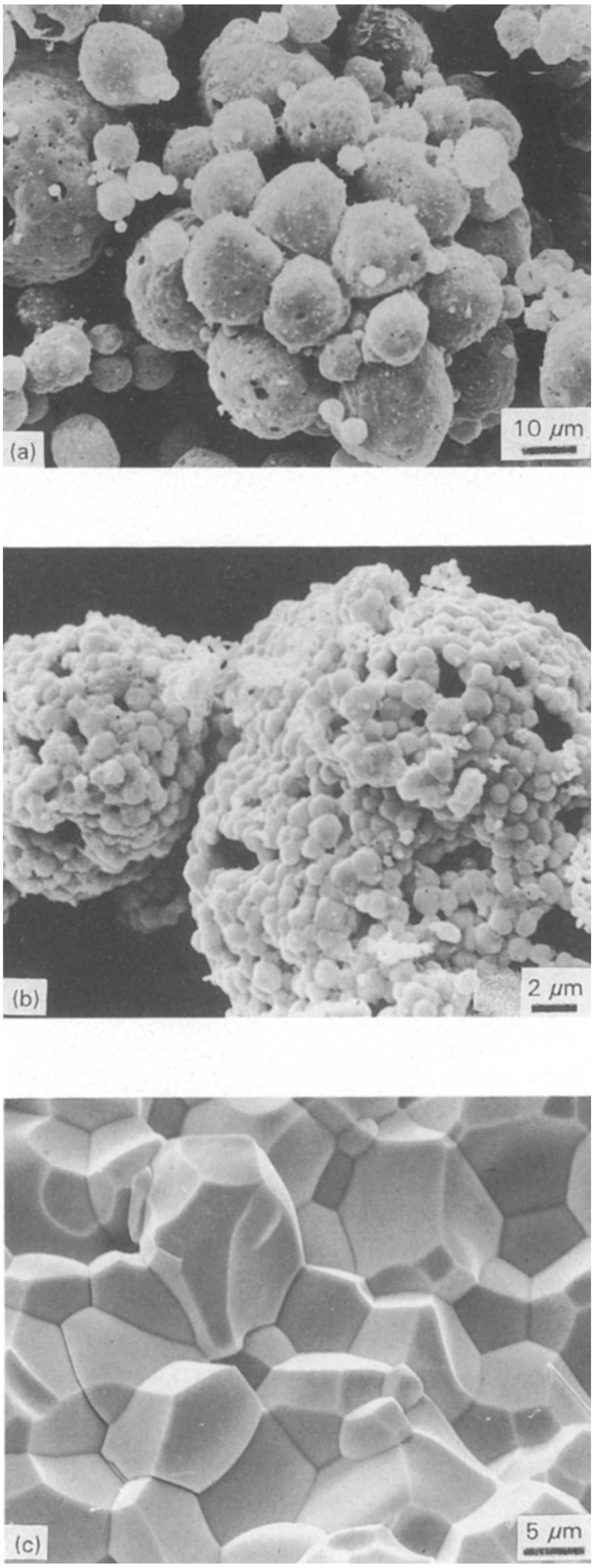

Figure 6 The morphology of: (a) as-sprayed powders, (b) calcined particles, and (c) the fractured surface of the specimen sintered at 1000 °C for 4 h.

to be obtainable when the 800 °C calcined powders were sintered at 1000 °C for 4 h. The granular structure was uniform, of 10 μm size, as shown in the micrograph of the fractured surface of the sintered specimens (Fig. 6c). The density was around 93% of TD.

The behaviour of sol–gel-derived powders has been observed to be rather significantly different from that of the other solution-derived powders. A series of thermal analyses such as TGA and DTA were thus performed to investigate the dissociation characteristics of spray-pyrolysed and sol–gel-derived powders. This was done to resolve this phenomena. In addition, FTIR spectra of the alkoxides, including $Mg(OEt)_2$, $Nb(OEt)_5$ and $Pb(CH_3COO)_2$, were examined before and after mixing.

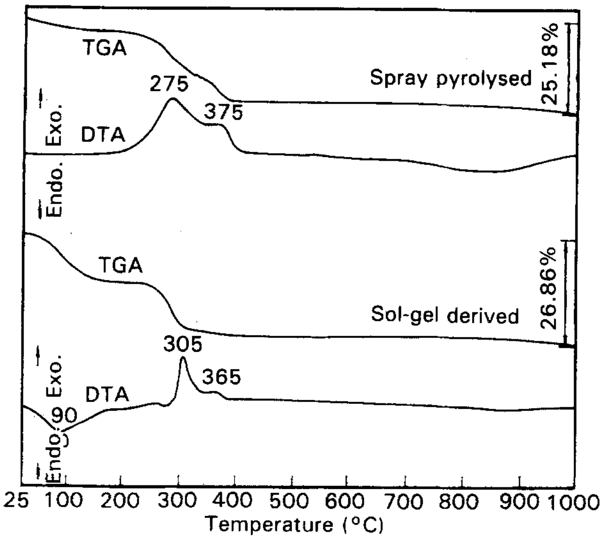

Figure 7 TGA–DTA curves of the spray-pyrolysed and sol–gel-derived powders. (Heating rate, 5 °C min^{-1}.)

Both the spray-pyrolysed and sol–gel-derived powders are indicated by the TGA and DTA curves shown in Fig. 7 to be dissociated by two major steps. The exothermic peaks which occurred at 275 °C and 375 °C are indicated by the corresponding data curve to be quite broad for spray-pyrolysed powders. These peaks correspond to the oxidation of the residual hydrocarbons. They are probably broad because of the randomness in the length of the hydrocarbon chain charred in the pyrolysing tube, since oxidization was initiated at different temperatures. On the other hand, the reactions occurred at 305 °C and 365 °C, besides the dissociation of entrapped solvent such as alcohol, 2-methoxyethanol, at 90 °C, for the sol–gel-derived powders. Most of the organic ligand is indicated by the sharp peak in the DTA curve to dissociate at the same temperature. The former peak (305 °C) was assigned to the dissociation of the OR ligand attached to Mg^{2+} and Nb^{5+} ions [21]. The small peak occurring at 365 °C possibly comes from another species, in a small amount, and can thus be assigned to the dissociation of the OAc ligand attached to the Pb^{2+} ions. That is, two categories of clusters, one corresponding to the RO–Mg–O–Nb–OR clusters and the other corresponding to the Pb–OAc clusters, are possibly formed in the gels derived from alkoxide precursors.

The FTIR spectra of the dried $Mg(OEt)_2$, $Nb(OEt)_5$, $Pb(OAc)_2$ gels and their mixtures were measured, and the results are shown in Fig. 8. The 1024 and 1071 cm^{-1} peaks observed in the $Nb(OEt)_5$ spectrum (Fig. 8b) were assigned, respectively, to vibrational absorption of asymmetric, (ν_{as}), and symmetric, ν_s, C–O–Nb bonds [25]. The 1024 cm^{-1} peak

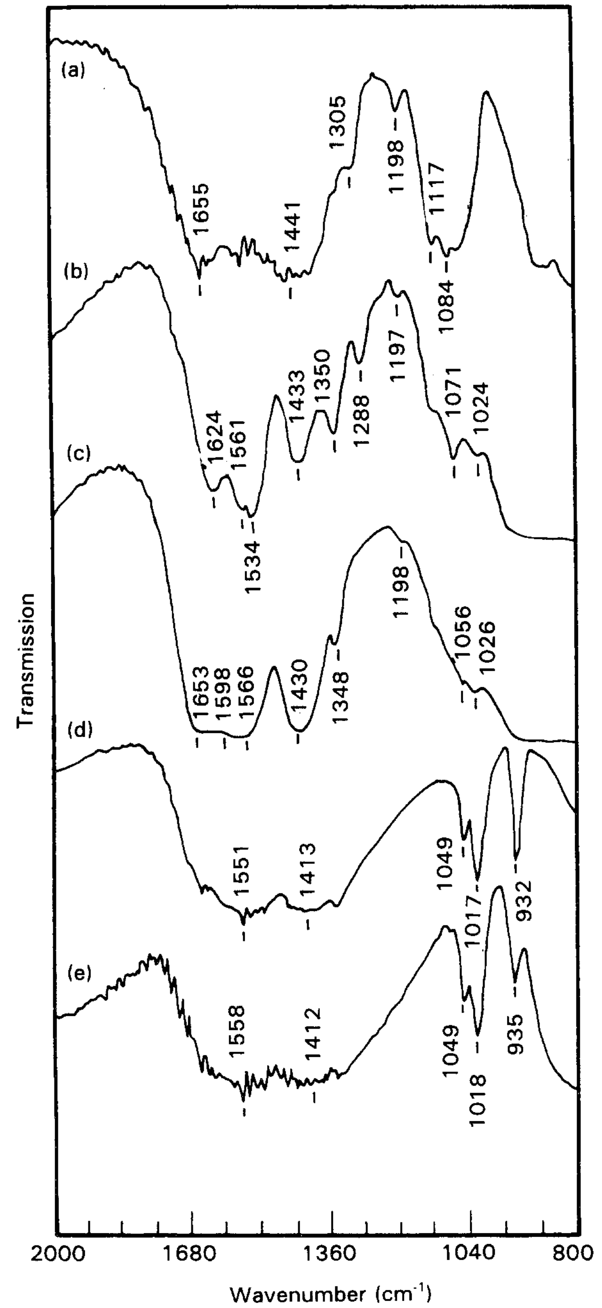

Figure 8 The FTIR spectra of the sol–gel starting materials: (a) $Mg(OEt)_2$, (b) $Nb(OEt)_5$, (c) $Mg(OEt)_2 + Nb(OEt)_5$, (d) $Pb(OAc)_2$, and (e) $Mg(OEt)_2 + Nb(OEt)_5 + Pb(OAc)_2$ refluxed in 2-methoxyethanol.

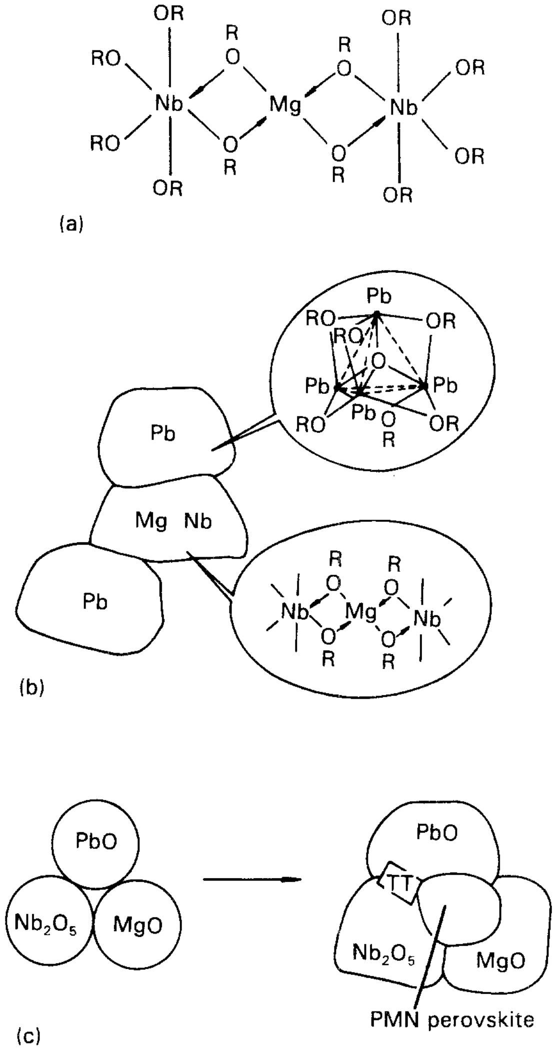

Figure 9 Schematic representation of: (a) the Mg, Nb double alkoxide [26], (b) the Pb cluster around the Mg, Nb cluster, and (c) the reaction of mixed oxides.

of the corresponding spectrum for the gels derived from the mixture of $Mg(OEt)_2$ and $Nb(OEt)_5$ did not shift at all, but the 1071 cm^{-1} peak shifted significantly to 1056 cm^{-1} (Fig. 8c). The double alkoxide could thus be assumed to have formed with the possible structure [26] shown in Fig. 9a; this occurred during the reflux of the $Mg(OR)_2$–$Nb(OR)_5$ mixture.

The 1084 cm^{-1} and 1117 cm^{-1} peaks of the $Mg(OR)_2$ gel were insufficiently weak to be resolved in the mixture. However, some modification apparently occurred to the ν_{as} and ν_s peaks of the $Mg(OR)_2$ spectrum. The other peaks, besides the (C–O) M peaks, are possibly due to the vibration of hydrocarbon–oxygen bonds. The 932 cm^{-1}, 1017 cm^{-1} and 1049 cm^{-1} peaks, which are possibly due to C–O–Pb vibrations, were observed in the $Pb(OAc)_2$ spectrum (Fig. 8d) to have hardly shifted at all when $Pb(OAc)_2$ is dissolved in the $Mg(OR)_2$–$Nb(OR)_5$ mixture, as shown in Fig. 8e. This implies that $Pb(OAc)_2$ did not form a multiple alkoxide with the Mg and Nb alkoxides. A Pb–O–Pb cluster structure, like lead alkoxide which underwent self-condensation to become a tetranuclear cluster [27], might occur. That is, the Pb–O–Pb clusters depicted in Fig. 9b are assumed to form, surrounding the Mg–O–Nb clusters.

4. Discussion

Both the freeze-drying and the spray-pyrolysis techniques are capable of synthesizing PMN materials free of the pyrochlore phase, at a rather low temperature. These materials can still be easily converted into the perovskite phase during sintering, even though the pyrochlore phase (π) is present after calcination. On the contrary, an appreciable amount of pyrochlore phase still remains after sintering when the materials are synthesized via the sol–gel route. This difficulty in synthesizing a pure perovskite phase, due to the formation of a pyrochlore phase (π-phase), is similar to the phenomenon observed in the mixed-oxide method.

The particle size of the starting materials, i.e. PbO, MgO and Nb_2O_5 powders, in the mixed-oxide process is usually a few micrometres. Pyrochlore (π) phases inevitably result at the interface of PbO and Nb_2O_5 particles during the calcination process with the formation of a PMN perovskite phase at the junctions of PbO–MgO–Nb_2O_5 particles, as depicted in Fig. 9c. Transformation of the π-phase particles into the perovskite phase requires the Mg^{2+} ions to diffuse all the way through the other oxide particles to this region. The pyrochlore phase formed is thus extremely difficult to eliminate, even after repeated firing for a prolonged period at an elevated temperature.

On the other hand, the solution mixing of cations is highly homogeneous and the pyrochlore particles formed are only of the scale of a few unit cells. The transformation of pyrochlore particles into a perovskite phase will only involve the diffusion of cations along a distance of only a few lattice parameters, and it is, therefore, quite feasible. In the sol–gel process, although the solution mixing of cations is highly homogeneous, the pyrochlore phases having formed preferentially can still not be converted into the perovskite phase even when sintered at high temperature. The pyrochlore particles formed in this process are inferred from this phenomena to be of a significant size.

This is in conformity with the observation from the TGA/DTA and FTIR analysis, in which the co-existence of $Pb(OAc)_2$ and Mg–O–Nb–OR clusters is clearly inferred. The Pb–O–Pb clusters surrounding the Mg–O–Nb clusters might possibly be of an appreciable size. The pyrochlore particles formed at the interface of large Pb–O clusters and Mg–O–Nb clusters might be sufficiently separated so as not to be converted into a perovskite phase in a finite sintering interval. A deleterious effect due to inhomogeneous mixing is observed, that is, the hydrolysis reaction in the sol–gel process which results in the separation of Pb^{2+}-cations from the Mg^{2+}–O–Nb^{5+} mixture is responsible for the formation of a pyrochlore phase which cannot be eliminated. On the other hand, the homogeneous mixing in the solution is preserved without separation during the freeze-drying or spray-pyrolysing process. The pyrochlore-phase particles are expected to be very fine and easy to transform into a perovskite phase.

As to the comparison between the two DSS methods, the advantage of the freeze-drying technique is that the agglomerates obtained are slightly smaller and are well separated. This is due to the fact that the cations are frozen inside the ice particles and are not brought into contact with each other while the ice molecules are sublimated. The slowness of this sublimation process and the expense of the apparatus are the disadvantages of this technique. The spray-pyrolysis technique, on the other hand, is a fast process. It takes only seconds to spray the solution into the hot zone to pyrolyse the atomized mist. Atomized droplets usually result in larger agglomerates, which is the advantage of this technique. This is not desirable in the preparation of high-sinterability powders. The agglomeration itself is, however, loose, and it can possibly be disintegrated by milling before calcination. Direct spray pyrolysis from solution can, therefore, be concluded to be a more promising technique for preparation of pyrochlore-free and high-sinterability perovskite PMN materials.

5. Conclusions

1. The powders were of amorphous form when the PMN solution was either prepared by the sol–gel, freeze-drying or spray-pyrolysis methods. These powders could be transformed into the desired perovskite phase by a calcination process.
2. A pyrochlore phase inevitably resulted during calcination of the as-dried powders. This phase could be completely eliminated for powders derived from freeze-drying or spray-pyrolysis routes. The conversion from the pyrochlore to the perovskite phase could not, however, be completed for sol–gel-derived powders.
3. The formation of $Pb(OAc)_2$ clusters accompanied by Mg–O–Nb double-alkoxide clusters, identified using TGA/DTA and FTIR techniques, is assumed to be the mechanism which results in pyrochlore particles which cannot be eliminated in the powders prepared via the sol–gel process.

Acknowledgement

The authors would like to express their gratitude to the National Science Council for financial support under contract no. NSC80-0404-E007-10.

References

1. S. L. SWARTZ, T. R. SHROUT, W. A. SCHULZE and L. E. CROSS, *Amer. Ceram. Soc. J.* **67** (5) (1984) 311–15.
2. V. A. BOKOV and I. E MYL'NIKOVA, *Sov. Phys. Solid State* **2** (1961) 2438–32.
3. G. A. SMOLENSKII and A. I. AGRANOVSKAYA, *Sov. Phys. Solid State* **1** (1960) 1429–37.
4. S. L. JANG, K. UCHINO, S. NOMURA and L. E. CROSS, *Ferroelectrics* **27** (1980) 31–34.
5. L. E. CROSS, S. J. JANG, R. E. NEWNHAM, S. NOMURA and K. UCHINO, *Ferroelectrics* **23** (1980) 187–92.
6. K. UCHINO, S. NOMURA, L. E. CROSS, S. L. JANG and R. E. NEWNHAM, *J. Appl. Phys.* **51** (1980) 1142–45.
7. SHOICHIRO NOMURA and KENJI UCHINO, *Ferroelectrics* **41** (1982) 117–32.
8. DINESH K. AGRAWAL, R. ROY and H. A. MCKINSTRY, *Mater. Res. Bull.* **22** (1987) 83–88.
9. L. A. SHEBANOV, P. P. KAPOSTINS and J. A. ZVIRGZDS, *Ferroelectrics* **56** (1984) 53–56.
10. D. J. VOSS, S. L. SWARTZ and T. R. SHROUT, *Ferroelectrics* **50** (1983) 203–208.
11. M. LEJEUNE and J. P. BOILOT, *Ferroelectrics* **54** (1984) 191–94.
12. S. L. SWARTZ and T. R. SHROUT, *Mater. Res. Bull.* **17** (1982) 1245–50.
13. J. P. GUHA and H. U. ANDERSON, *Amer. Ceram. Soc. J.* **69** (11) (1986) C287–88.
14. A. KATO, *Indust. Ceram.* **7** (2) (1987) 105–8.
15. D. W. JOHNSON, Jr, *Amer. Ceram. Soc., Bull.* **60** (1981) 221–43.
16. P. A. LESSING, *Amer. Ceram. Soc., Bull.* **68** (1989) 1002–7.
17. H. U. ANDERSON, M. J. PENNELL and J. P. GUHA, *Advan. Ceram.* **21** (1987) 91–98.
18. T. FUKUI, C. SAKURAI and M. OKUYAMA, *J. Non-cryst. Solids* **134** (1991) 293–295.
19. P. RAVINDRANATHAN, S. KOMARNENI, A. S. BHALLA, R. ROY and L. E. CROSS, *Ceram. Trans.* **1** (1988) 182–9.

20. P. RAVINDRANATHAN, S. KOMARNENI and R. ROY, *Amer. Ceram. Soc., J.* **73** (1990) 1024–25.
21. F. CHAPUT, J. P. BOILOT, M. LEJEUNE, R. PAPIERNIK, and L. G. HUBERT-PFALZGRAF, *Amer. Ceram. Soc. J.* **72** (1989) 1355–57.
22. D. C. BRADLEY, B. N. CHAKRAVARTI, and W. WARDLAW, *J. Chem. Soc.* (1956) 2381–84.
23. KOICHI, Japanese Patent 8 636 107, 20 February (1986).
24. M. PECHINI, US Patent 3 330 697, 11 July (1967).
25. D. C. BRADLEY, R. C. MEHROTRA and D. P. GAUR, in "Metal alkoxides", (Academic Press, London, 1978) p. 116.
26. S. GOEL and A. B. GOEL and B. C. MEHOTRA, *Syn. React. Inorg. Metal-Org. Chem.* **6** (4) (1976) 251–263.
27. R. PAPIERNIK, L. G. HUBERT-PFALZGRAF and MARIE-CECILE MASSIANI, *Inorg. Chim. Acta* **165** (1989) 1–2.

Received 21 October 1992
and accepted 24 February 1993